Bayesian Pulse Shape Inference for TES-Based Cryogenic Calorimeters

Sarah Braun on behalf of the COSINUS collaboration

Pulse shapes encode phonon transport: BAT.jl inference extracts interface-specific parameters and locates detector bottlenecks.

1) Measured TES pulse → 2) Physical pulse shape model → 3) BAT.jl Bayesian inference → 4) Interface-specific detector parameters → 5) Detector comparison and optimization

Detector physics and model

1) Detector concept

COSINUS uses NaI crystals as **cryogenic, scintillating calorimeters** to test the DAMA/LIBRA annual-modulation claim with the same target material. Since direct TES fabrication on NaI is not feasible, COSINUS uses the **remoTES** design. The relevant signal path is:
Absorber → Metallic collector/link → TES → Bath
The measured pulse depends on how efficiently energy crosses the absorber–collector and collector–TES interfaces.

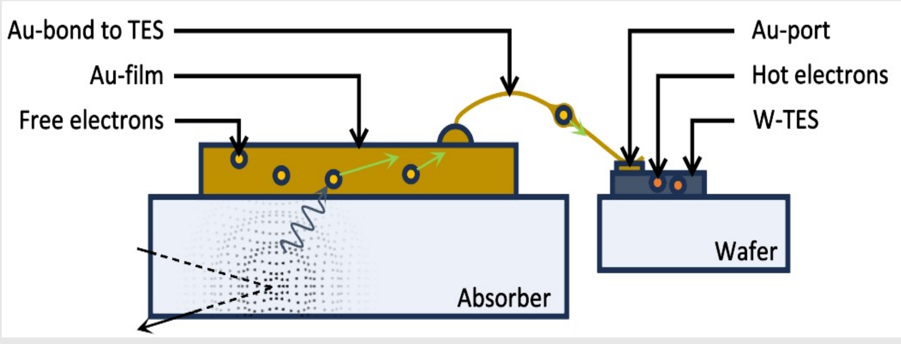

2) Signal formation

A particle hit creates **athermal phonons** in the absorber. A fraction η of this athermal phonon energy reaches the metallic collector. In the metal, phonon energy is transferred to the electronic system by **electron-phonon coupling**.
The collector-side electronic energy then splits effectively:

- ε: Prompt transfer to TES
- (1-ε): Delayed detector response

The remaining absorber energy (1- η) **thermalizes** in the absorber and contributes to slower pulse components. The delayed components reach the TES through the thermal conductances G_{ag} and G_{eg}.

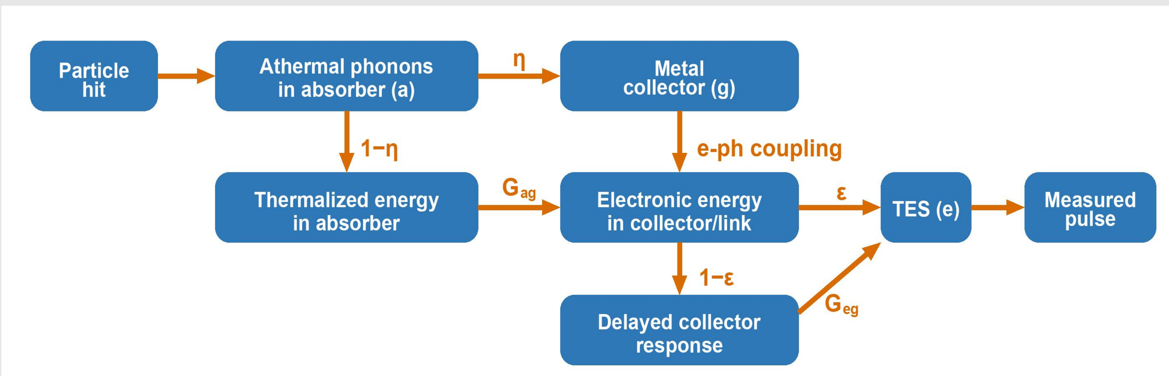

3) Thermal model and fit parameters

The remoTES pulse shape is modeled by three coupled thermal nodes:
a = absorber, g = collector/link, e = TES
The temperature evolution is described by

$$C_i \dot{T}_i + \sum_j G_{ij}(T_i - T_j) = P_i(t)$$

where C_i is the heat capacity, G_{ij} the thermal conductance and $P_i(t)$ the power input from the athermal phonons. The measured waveform is proportional to the **TES temperature response $\Delta T_e(t)$.**

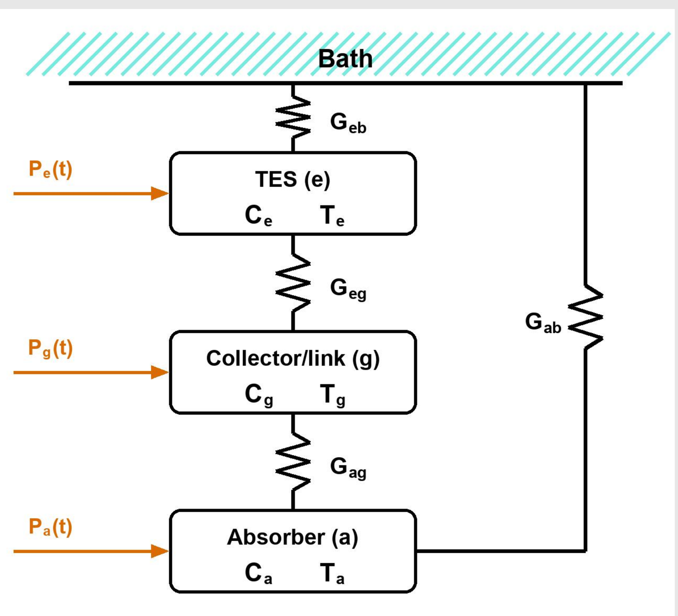

Fit parameter	Physical meaning	Interface / Component
G_{ag}/C_a	Thermal response rate	Absorber → Collector
G_{eg}/C_g	Thermal response rate	Collector → TES
G_{eb}/C_e	Thermal response rate	TES → Bath
η	Athermal collection efficiency	Absorber → Collector
ε	Prompt energy-transfer efficiency	Collector/link → TES
$\tau_{crystal}$	Athermal phonon lifetime	Absorber
$\tau_{collector}$	Delayed collector response time	Collector/link
τ_{film}	TES-side thermalization time	TES

Bayesian framework and model comparison

4) Bayesian pulse shape inference

Cleaned pulses are averaged into a noise-reduced **standard event** and fitted with the physical pulse shape model.

The model parameters are strongly correlated, motivating a Bayesian treatment of uncertainties and correlations. The inference framework is implemented with BAT.jl.

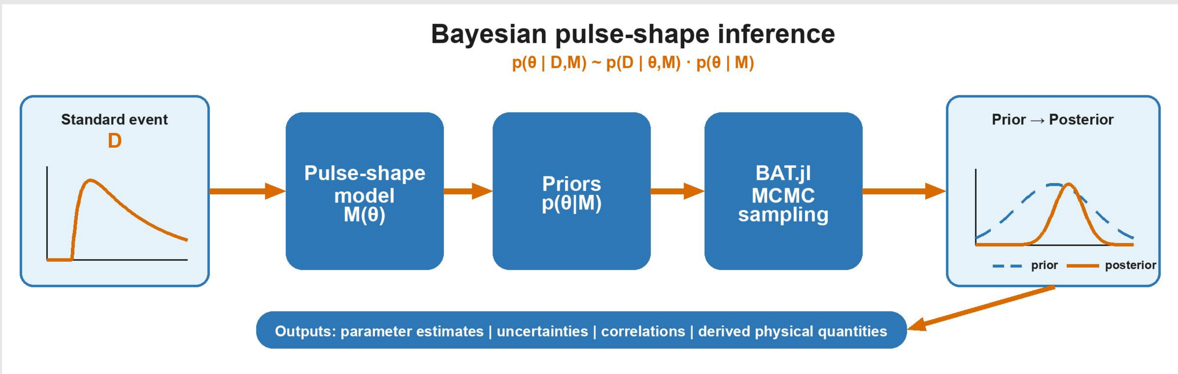

5) Likelihood tempering

Standard events are averages of many pulses and therefore have strongly reduced noise. The resulting likelihood can become very narrow and difficult to sample.
To stabilize the inference, the fit is performed iteratively: an enlarged noise parameter σ is used first and then gradually reduced to the physical baseline RMS.

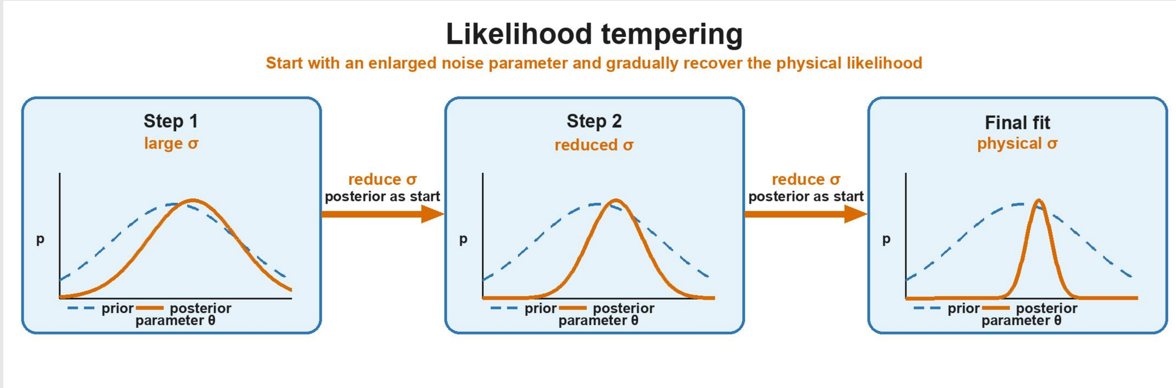

6) Model comparison

One key question is whether the collector/link can be absorbed into the TES node or must be modeled independently.

Model	Thermal nodes	Interpretation
2-component	a + e	collector/link follows TES instantly
3-component	a + g + e	collector/link has its own thermal response

Bayesian and frequentist model-comparison tests consistently favor the three-component model for remoTES standard events.

The collector/link has its own thermal response.

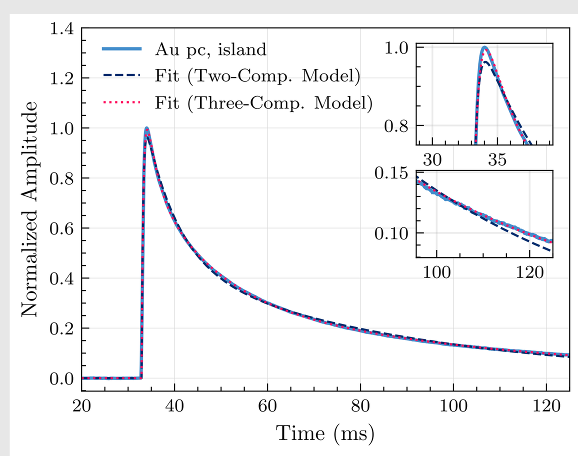

7) Interface-specific interpretation

The three-component model separates the two signal-transfer steps:
a → g and g → e
Pulse shape inference identifies the limiting detector interface.

Fit signature	Interpretation
low η, small G_{ag}/C_a	Absorber–collector bottleneck
low ε, small G_{eg}/C_g	Collector–TES bottleneck
large $\tau_{collector}$	Delayed collector response
large τ_{film}	Slow transfer into TES signal
long $\tau_{crystal}$	Athermal phonons survive longer in absorber

This enables detectors to be compared through physical transport parameters, not only through energy resolution.

Results and detector comparison

8) Si remoTES design comparison

Three Si prototypes are used as a controlled testbed for the remoTES signal path
a → g → e.

Detector	Design	Purpose
Si-1	Au collector + Au bridge TES	Reference
Si-2	Same Au collector + Au island TES	Test eg-interface
Si-3	Cu collector + same Au island TES	Test ag-interface

Au bridge: Au port contacts wafer and TES.
Au island: Au port is only on the TES film, reducing parasitic contact to the wafer.
The temperature evolution plots are calculated from the fitted three-component model parameters and show where energy is stored or delayed.

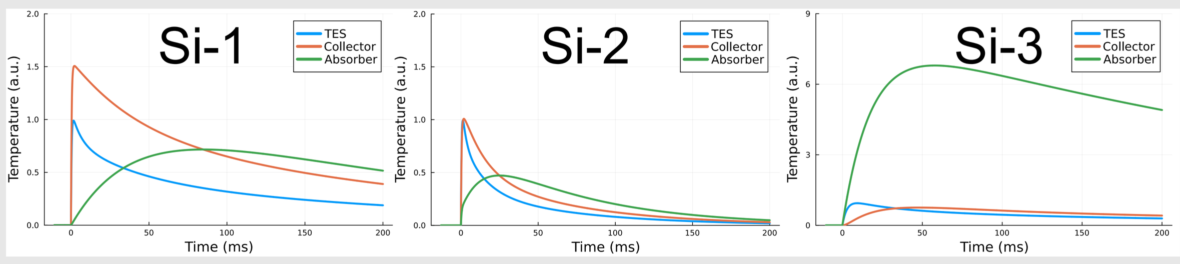

9) What the fitted parameters show

Green cells: **Si-1** → **Si-2**, testing Au bridge → Au-island TES
Yellow cells: **Si-2** → **Si-3**, testing Au → Cu collector

Parameter	Si-1	Si-2	Si-3
G_{eg}/C_g (ms^{-1})	0.013	0.085	0.049
ε	0.105	0.335	0.990
$\eta\varepsilon$	0.105	0.311	0.361
τ_{film} (ms)	3.90	1.29	18.7
G_{ag}/C_a (ms^{-1})	0.0165	0.0376	0.0029
η	0.998	0.930	0.365
$\tau_{crystal}$ (ms)	251	8.85	1052
$\tau_{collector}$ (ms)	0.45	0.64	1828

The Au island improves the collector–TES side:
$G_{eg}/C_g \uparrow$, $\varepsilon \uparrow$, $\eta\varepsilon \uparrow$, $\tau_{film} \downarrow$
Au island improves g → e coupling

For the Cu collector, the long $\tau_{crystal}$ is compatible with improved athermal phonon survival. The low η, small G_{ag}/C_a and long $\tau_{collector}$ indicate inefficient conversion/collection in the Cu collector. Possible reasons include weaker ep-coupling and an imperfect Cu film.

Comparison	Observation	Interpretation
Si-1 → Si-2	faster collector/TES response	Au island improves $g \to e$
Si-2 → Si-3	dominant absorber response	Cu changes athermal dynamics but limits $a \to g$

10) Conclusions and Outlook

Pulse shape inference converts pulse shapes into detector-physics parameters.
The BAT.jl framework extracts thermal response rates, collection efficiencies, and decay times, allowing detector bottlenecks to be localized interface by interface.
This enables detector designs to be compared through physical transport parameters, not only through energy resolution.
The method is transferable to TES-based cryogenic calorimeters beyond COSINUS.

Future direction: Fast **per-event inference** to scale the method from standard-event fits to high-statistics cryogenic detector data.

COLLABORATION

IDM2026, ZARAGOZA

Contact: sarah.braun@oeaw.ac.at

cosinus.it